Analytical modeling of potential distribution in Trigate SOI MOSFETs

Hamdam Ghanatian [1]
Electrical Engineering Department
Ferdowsi University of Mashhad
Mashhad, Iran.
Ghanatian.hamdam@stu.um.ac.ir

Seyed Ebrahim Hosseini [2]
Electrical Engineering Department
Ferdowsi University of Mashhad
Mashhad, Iran.
ehosseini@um.ac.ir

Abstract— In this paper a new 3-D analytical model for the potential distribution in nano-scaled lightly doped trigate silicon on insulator MOSFETs in the subthreshold regime, is proposed. This model is derived by solving 3-D Poisson' s equation and using parabolic potential distribution assumption between lateral gates. The proposed analytic model is investigated and compared with the obtained results from 3-D simulations using ATLAS device simulator. It is demonstrated that analytic solution has a good accuracy to predict potential distribution along the silicon body.

Keywords— analitical model; trigate SOI MOSFET; 3-D Poisson's equation; parabolic potential distribution.

I. INTRODUCTION

Device architectures based on Silicon-On-Insulator (SOI) technology, i.e., ultra-thin body SOI transistors, double gate (DG) and trigate (TG) SOI MOSFET are candidates for extension of CMOS scaling beyond the limits set for the bulk transistors [1-2]. These devices can operate in fully depleted (FD) regime and thus provide reduced short channel effects, leakage current and maintain good scaling capability [3-4].TG transistors are more interesting as compared to DG transistors for scaling because the 3-D structure of TG SOI MOSFETs redounds to improve control of the gate over the entire channel, therefore the short channel problems are less than those in DG SOI MOSFETs [5-6]. The TG MOSFETs are being used by Intel because of high I_{on}/I_{off} [7]. The body of these transistors are usually lightly doped, because the body scattering effects are reduced that lead to increase the carrier mobility and derive current [8 For obtaining an analytical solution based on gradual channel approximation (GCA) [9] in DG transistors, 3-D Poisson' s equation can be reduced to 1-D equations because of their symmetric structures. Although, in TG SOI MOSFETs due to asymmetric structures, finding an analytical solution directly is so challenging and more approximations are required [10-12]. In order to obtain an analytical model for potential distribution along the channel for TG MOSFET, in [13] 2-D Poisson' s equation in symmetry and asymmetry DG MOSFET is solved separately and the total potential for TG MOSFET is produced by adding the obtained potential in symmetry and asymmetry DG MOSFET based on perimeter-weighted approximation In [14] 3-D Poisson' s equation is solved by using 1-D Poisson' s equation and 3-D Laplace equation in TG SOI MOSFET. The obtained potential is independent of the drain voltage. In this paper, alternative and simple analytic model for potential distribution is investigated based on solving 3D Poisson' s equation in lightly doped TG in subthreshold regime. This model is explicit and dependent on the drain voltage. The achieved body potential has been verified by comparison with the results obtained from 3-D numerical device simulations.

II. DESCRIPTION OF MODEL

The schematic of the cross-sectional view of TG SOI MOSFET is given in Fig. 1.

Fig. 1. The schematic cross-sectional view of trigate SOI MOSFET. t_{ox} and t_{oxb} are thicknesses of the gate oxide and buried respectively.

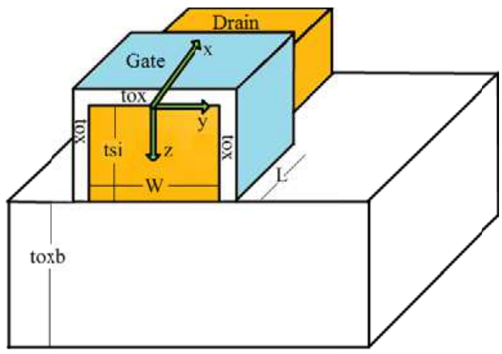

The potential distribution along the channel, $\varphi(x,y,z)$, is derived by solving the 3D Poisson's equation.

$$\frac{d^2\varphi(x,y,z)}{dx^2}+\frac{d^2\varphi(x,y,z)}{dy^2}+\frac{d^2\varphi(x,y,z)}{dz^2}=\frac{qN_A}{\varepsilon_{si}} \quad (1)$$

$0\leq x\leq W/2$, $-W/2\leq y\leq t_{si}$, $0\leq z\leq L$

Where N_A is the channel dopant concentration and ε_{si} is the dielectric constant of silicon. The potential between the lateral gates is assumed parabolic [15-16].

$$\varphi(x,y,z)\approx a_0(x,z)+a_1(x,z)y+a_2(x,z)y^2 \quad (2)$$

In low drain voltage, the potential distribution is parabolic function in the z-direction [17]. At y=0, the potential distribution is as follows:

$$\varphi(x,0,z) = a_0(x,z) \approx C_0(x) + C_1(x)z + C_2(x)z^2 \tag{3}$$

The potential at front, lateral (φ_f) and back (φ_{sb}) interfaces are:

$$\varphi(x,0,0) = \varphi_f(x) = a_0(x,0) = c_0(x) \tag{4}$$

$$\varphi(x,0,t_{si}) = \varphi_{sb}(x) = a_0(x,t_{si}) = C_0(x) + C_1(x)t_{Si} + C_2(x)t_{Si}^2 \tag{5}$$

And because of symmetry along y coordinate:

$$\varphi(x,-\frac{w}{2},z) = \varphi\left(x,\frac{w}{2},z\right) \tag{6}$$

From equation (6) the coefficient, $a_1(x, z)$ is zero, therefore:

$$\varphi(x,\pm\frac{w}{2},z) = \varphi_f(x) = a_0(x,z) + a_2(x,z)\frac{w^2}{4} \tag{7}$$

By using Gauss' law in z-direction, the boundary conditions at the channel-oxide interface are:

$$C_1(x) = \left.\frac{d\varphi}{dz}\right|_{y=0,\,z=0} = \frac{\varepsilon_{ox}}{\varepsilon_{Si}}\frac{\varphi_f(x) - V'_{gs}}{t_{ox}} \tag{8}$$

$$C_1(x) + 2C_2(x)t_{Si} = \left.\frac{d\varphi}{dz}\right|_{y=0,\,z=t_{Si}} = \frac{\varepsilon_{ox}}{\varepsilon_{Si}}\frac{V'_{sub} - \varphi_{sb}}{t_{oxb}} \tag{9}$$

Where $V'_{gs} = V_g - V_{FB1}$, $V'_{sub} = V_{sub} - V_{FB2}$ that V_g and V_{sub} are the top and bottom gate voltages respectively and ε_{ox} is the constant of the oxide. The V_{FB1} and V_{FB2} are the top and bottom gate flat-band voltages respectively. The flat-band voltage is $V_{FB} = \frac{-kT}{q}\ln(N_A / n_i)$ for mid-gap gate material that $\frac{kT}{q}$ is the thermal voltage and n_i is the intrinsic carrier concentration. By using (8), (9) c_2 is obtained and expressed through φ_f .

$$C_2(x) = \frac{\frac{\varepsilon_{ox}}{\varepsilon_{si}t_{oxb}}V'_{sub} - \varphi_f\left[\frac{\varepsilon_{ox}}{\varepsilon_{si}t_{ox}}\left(1+\frac{\varepsilon_{ox}t_{si}}{\varepsilon_{si}t_{oxb}}\right) + \frac{\varepsilon_{ox}}{\varepsilon_{si}t_{oxb}}\right] + \frac{\varepsilon_{ox}}{\varepsilon_{si}t_{ox}}\left(1+\frac{\varepsilon_{ox}t_{si}}{\varepsilon_{si}t_{oxb}}\right)V'_{gs}}{\left[2t_{si} + \frac{\varepsilon_{ox}t_{si}^2}{\varepsilon_{si}t_{oxb}}\right]} \tag{10}$$

By considering (7), the coefficient a_2 is (11):

$$a_2(x,z) = \frac{4}{w^2}\left[\varphi_f(x) - a_0(x,z)\right] \tag{11}$$

By substituting the coefficients in (2), the 3D potential distribution is achieved in (12).

$$\begin{aligned}\varphi(x,y,z) = {} & \varphi_f(x) + \left(\frac{\varepsilon_{ox}}{\varepsilon_{Si}}\frac{\varphi_f(x) - V'_{gs}}{t_{ox}}\right)z + \left(\frac{\frac{\varepsilon_{ox}}{\varepsilon_{si}t_{oxb}}V'_{sub} - \varphi_f\left[\frac{\varepsilon_{ox}}{\varepsilon_{si}t_{ox}}\left(1+\frac{\varepsilon_{ox}t_{si}}{\varepsilon_{si}t_{oxb}}\right) + \frac{\varepsilon_{ox}}{\varepsilon_{si}t_{oxb}}\right] + \frac{\varepsilon_{ox}}{\varepsilon_{si}t_{ox}}\left(1+\frac{\varepsilon_{ox}t_{si}}{\varepsilon_{si}t_{oxb}}\right)V'_{gs}}{\left[2t_{si} + \frac{\varepsilon_{ox}t_{si}^2}{\varepsilon_{si}t_{oxb}}\right]}\right)z^2 \\ & - \frac{4}{w^2}\left(\left(\frac{\varepsilon_{ox}}{\varepsilon_{Si}}\frac{\varphi_f(x) - V'_{gs}}{t_{ox}}\right)z + \frac{\frac{\varepsilon_{ox}}{\varepsilon_{si}t_{oxb}}V'_{sub} - \varphi_f\left[\frac{\varepsilon_{ox}}{\varepsilon_{si}t_{ox}}\left(1+\frac{\varepsilon_{ox}t_{si}}{\varepsilon_{si}t_{oxb}}\right) + \frac{\varepsilon_{ox}}{\varepsilon_{si}t_{oxb}}\right] + \frac{\varepsilon_{ox}}{\varepsilon_{si}t_{ox}}\left(1+\frac{\varepsilon_{ox}t_{si}}{\varepsilon_{si}t_{oxb}}\right)V'_{gs}}{\left[2t_{si} + \frac{\varepsilon_{ox}t_{si}^2}{\varepsilon_{si}t_{oxb}}\right]}z^2\right)y^2\end{aligned} \tag{12}$$

The differential equation for the surface potential is obtained by inserting (12) in (1), which is given by (13):

$$\frac{d^2\varphi_f(x)}{dx^2} - \alpha\varphi_f(x) = \beta \tag{13}$$

Where

$$\alpha = \frac{\frac{8}{w^2}\left(\frac{\varepsilon_{ox}}{\varepsilon_{Si}t_{ox}}z - Az^2\right) + 2A - \frac{8}{w^2}y^2A}{1 + \frac{\varepsilon_{ox}}{\varepsilon_{si}t_{ox}}z - Az^2 - \frac{4}{w^2}\frac{\varepsilon_{ox}}{\varepsilon_{si}t_{ox}}zy^2 + \frac{4}{w^2}Az^2y^2} \tag{14}$$

$$\begin{aligned}\beta = {} & \frac{\frac{qNA}{\varepsilon_{si}} + \frac{8}{w^2}\left(\left(\frac{\varepsilon_{ox}}{\varepsilon_{Si}}\frac{-V'_{gs}}{t_{ox}}\right)z + \frac{\frac{\varepsilon_{ox}}{\varepsilon_{si}t_{oxb}}V'_{sub} + \frac{\varepsilon_{ox}}{\varepsilon_{si}t_{ox}}\left(1+\frac{\varepsilon_{ox}t_{si}}{\varepsilon_{si}t_{oxb}}\right)V'_{gs}}{\left[2t_{si} + \frac{\varepsilon_{ox}t_{si}^2}{\varepsilon_{si}t_{oxb}}\right]}z^2\right) -}{1 + \frac{\varepsilon_{ox}}{\varepsilon_{si}t_{ox}}z - Az^2 - \frac{4}{w^2}\frac{\varepsilon_{ox}}{\varepsilon_{si}t_{ox}}zy^2 + \frac{4}{w^2}Az^2y^2} \\ & \frac{2\left(\frac{\frac{\varepsilon_{ox}}{\varepsilon_{si}t_{oxb}}V'_{sub} + \frac{\varepsilon_{ox}}{\varepsilon_{si}t_{ox}}\left(1+\frac{\varepsilon_{ox}t_{si}}{\varepsilon_{si}t_{oxb}}\right)V'_{gs}}{\left[2t_{si} + \frac{\varepsilon_{ox}t_{si}^2}{\varepsilon_{si}t_{oxb}}\right]}\right) + \frac{8}{w^2}y^2\left(\frac{\frac{\varepsilon_{ox}}{\varepsilon_{si}t_{oxb}}V'_{sub} + \frac{\varepsilon_{ox}}{\varepsilon_{si}t_{ox}}\left(1+\frac{\varepsilon_{ox}t_{si}}{\varepsilon_{si}t_{oxb}}\right)V'_{gs}}{\left[2t_{si} + \frac{\varepsilon_{ox}t_{si}^2}{\varepsilon_{si}t_{oxb}}\right]}\right)}{1 + \frac{\varepsilon_{ox}}{\varepsilon_{si}t_{ox}}z - Az^2 - \frac{4}{w^2}\frac{\varepsilon_{ox}}{\varepsilon_{si}t_{ox}}zy^2 + \frac{4}{w^2}Az^2y^2}\end{aligned} \tag{15}$$

$$A = \frac{\left[\frac{\varepsilon_{ox}}{\varepsilon_{si}t_{ox}}\left(1+\frac{\varepsilon_{ox}t_{si}}{\varepsilon_{si}t_{oxb}}\right) + \frac{\varepsilon_{ox}}{\varepsilon_{si}t_{oxb}}\right]}{\left[2t_{si} + \frac{\varepsilon_{ox}t_{si}^2}{\varepsilon_{si}t_{oxb}}\right]} \tag{16}$$

By using the boundary conditions as follows, equation (13) can be solved

$$\begin{gathered}\phi(0,y,z) = V_{bi} \\ \phi(L,y,z) = V_{bi} + V_{DS}\end{gathered} \tag{17}$$

Where V_{bi} is the built-in voltage ($V_{bi} = V_T Ln\left(N_A N_D / n_i^2\right)$) in which N_D is the source/drain doping concentration.

By solving (13) with the suitable boundary conditions in (18), the surface potential is obtained:

$$\varphi_f = -\sigma + \left[\frac{V_{bi}-D}{C} + \sigma - \frac{\frac{V_{bi}+V_{DS}-D}{C} + \sigma - \left(\frac{V_{bi}-D}{C}+\sigma\right)\exp(\Gamma)}{\exp(-\Gamma)-\exp(\Gamma)}\right]\exp\left((\alpha)^{1/2}x\right) + \left[\frac{\frac{V_{bi}+V_{DS}-D}{C} + \sigma_f - \left(\frac{V_{bi}-D}{C}+\sigma_f\right)\exp(\Gamma)}{\exp(-\Gamma)-\exp(\Gamma)}\right]\exp\left((\alpha)^{-1/2}x\right) \tag{18}$$

Where

$$C = 1 + k_1 z - k_4 z^2 - k_5 z y^2 + k_8 z^2 y^2$$
$$D = -k_2 z + k_3 z^2 + k_6 z y^2 - k_7 z^2 y^2 \tag{19}$$

The coefficients, k_1, k_2,..., k_8 are given in appendix. $\sigma \equiv \beta / \alpha$ and $\Gamma = L(\alpha)^{1/2}$.By replacing φ_f in (2), the 3-D potential distribution is obtained.

III. Results and Discussion

Fig.2 shows the potential distribution within the channel. This figure compares the obtained results from the analytical model with the simulation results. The front gate, back gate (substrate) and drain voltages are 0.2, 0 and 0.02 V respectively. The channel is lightly doped (donor concentration 10^{15} cm^{-3}), the n^+ source and drain are highly doped, and the dimensions of TG structure are as follows: buried-oxide thickness (t_{oxb}) = 100 nm, gate oxide thickness (t_{ox}) =1nm, t_{si}=5nm, W=5nm, L=15nm and the midgap gate material is applied. The simulation tool used in this study is Silvaco ATLAS [18]. The analytical model is classic model in which the quantum confinement [19] is neglected. It is observed that the results of the analytical model are verified with a good accuracy with the simulation results.

Fig. 2. The potential distribution in trigate SOI MOSFET while the gate, drain and substrate bias are 0.2, 0.02 and 0V respectively. The parameters of the transistor structure are t_{oxb}=100nm, t_{ox}=1nm, tsi=5nm, W=5nm, L=15nm.The potential is shown at different cut lines (a) y=0, z=2nm (b) y=0, z=5nm (c) y=2.5nm, z=2nm (d) y=2.5nm, z=5nm.

(a)

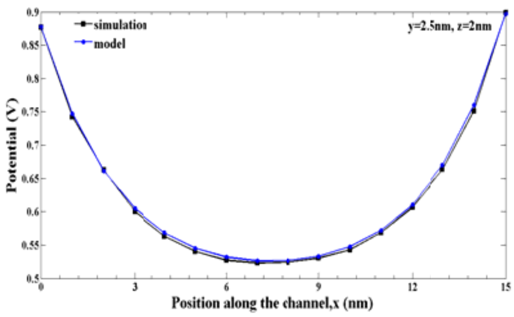

(b)

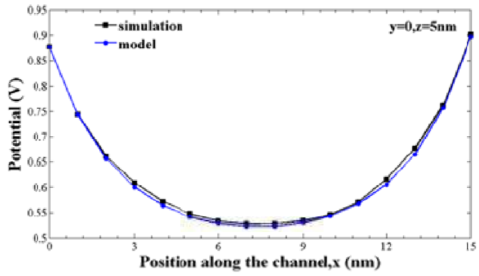

(c)

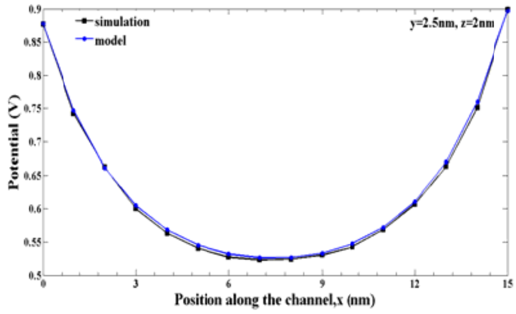

(d)

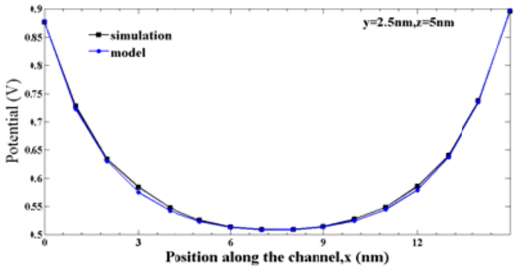

Fig.3 depicts, the potential distribution along the channel at the position z=2nm and y=0 with the drain voltages 0.4V and 1V, and the gate voltage 0.2V. It is observed that the results of the analytical model coincide with the simulation results for the different drain voltages.

Fig. 3. The potential distributions along the channel at y=0 and z=2nm .W, t_{si} and L are 5, 5, 15nm respectively. The drain voltages are applied 0.4V and 1V and the gate voltage is 0.2V.

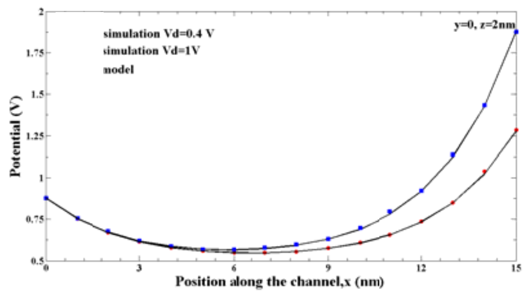

IV. Conclusion

By using the parabolic potential distribution assumption between two lateral gates and solving the 3D Poisson' s equation, a simple analytical model for the potential distribution in nano-scaled lightly doped trigate SOI MOSFET is obtained. This model is advantageous in explicit equation and good accuracy to predict potential through the transistor body.

APPENDIX

The coefficients, $k_1, k_2, \ldots, k_8$ are as follows:

$$k_1 = \frac{\varepsilon_{ox}}{\varepsilon_{Si} t_{ox}} \tag{A.1}$$

$$k_2 = \frac{\varepsilon_{ox} V'_{gs}}{\varepsilon_{Si} t_{ox}} \tag{A.2}$$

$$k_3 = \frac{\frac{\varepsilon_{ox}}{\varepsilon_{si} t_{oxb}} V'_{sub} + \frac{\varepsilon_{ox}}{\varepsilon_{si} t_{ox}} \left(1 + \frac{\varepsilon_{ox} t_{si}}{\varepsilon_{si} t_{oxb}}\right) V'_{gs}}{\left[2t_{si} + \frac{\varepsilon_{ox} t_{si}^2}{\varepsilon_{si} t_{oxb}}\right]} \tag{A.3}$$

$$k_4 = \frac{\left[\frac{\varepsilon_{ox}}{\varepsilon_{si} t_{ox}} \left(1 + \frac{\varepsilon_{ox} t_{si}}{\varepsilon_{si} t_{oxb}}\right) + \frac{\varepsilon_{ox}}{\varepsilon_{si} t_{oxb}}\right]}{\left[2t_{si} + \frac{\varepsilon_{ox} t_{si}^2}{\varepsilon_{si} t_{oxb}}\right]} \tag{A.4}$$

$$k_5 = \frac{4\varepsilon_{ox}}{w^2 \varepsilon_{Si} t_{ox}} \tag{A.5}$$

$$k_6 = \frac{4\varepsilon_{ox} V'_{gs}}{w^2 \varepsilon_{Si} t_{ox}} \tag{A.6}$$

$$k_7 = \frac{4}{w^2} \frac{\frac{\varepsilon_{ox}}{\varepsilon_{si} t_{oxb}} V'_{sub} + \frac{\varepsilon_{ox}}{\varepsilon_{si} t_{ox}} \left(1 + \frac{\varepsilon_{ox} t_{si}}{\varepsilon_{si} t_{oxb}}\right) V'_{gs}}{\left[2t_{si} + \frac{\varepsilon_{ox} t_{si}^2}{\varepsilon_{si} t_{oxb}}\right]} \tag{A.7}$$

$$k_8 = \frac{4}{w^2} \frac{\left[\frac{\varepsilon_{ox}}{\varepsilon_{si} t_{ox}} \left(1 + \frac{\varepsilon_{ox} t_{si}}{\varepsilon_{si} t_{oxb}}\right) + \frac{\varepsilon_{ox}}{\varepsilon_{si} t_{oxb}}\right]}{\left[2t_{si} + \frac{\varepsilon_{ox} t_{si}^2}{\varepsilon_{si} t_{oxb}}\right]} \tag{A.8}$$

References

[1] H. Iwai, “Roadmap for 22 nm and beyond,” Microelectron. Eng., vol. 86,no. 7–9, pp. 1520–1528, Jul.–Sep. 2009.

[2] N. Collaert, A. De Keersgieter, A. Dixit, I. Ferain, L.-S. Lai, D. Lenoble, A. Mercha, A. Nackaerts, H.-S.P. Wong , F .Boeuf., “Multi-gate devices for the 32 nm technology node and beyond, ” Solid-State Electronics., vol.52, pp.1291-1296,2008.

[3] J. P. Colinge, FinFETs and Other Multi-Gate MOSFETs. Berlin, Germany: Springer, 2008.

[4] A. Son, J. Kim, N. Jeong, J. Choi, and H. Shin, “Improved explicit current-voltage model for long-channel undoped surrounding-gate metal oxide semiconductor field effect transistor,” J. Appl. Phys., vol. 48, pp. 412–413, Apr. 2009.

[5] I. Ferain, C. Colinge, and J. Colinge, “Multigate transistors as the future of classical metal–oxide–semiconductor field-effect transistors,” Nature, vol. 479, no. 7373, pp. 310–316, Nov. 2011.

[6] J. Colinge, “Multiple-gate SOI MOSFETs,” Solid State Electron., vol. 48, no. 6, pp. 897–905, Jun. 2004.

[7] J. Cartwright, “Intel enters the third dimension,” Nature, 2011. doi: 10.1038/news.2011.274. [Online]. Available: http://www.nature.com/news/2011/110506/full/news.2011.274.html.

[8] T. Ghani, K. Mistry, P. Packan, S. Thompson, M. Stettler, S. Tyagi, and M. Bohr, “Scaling challenges and device design requirements for high performance sub 50 nm gate length planar CMOS transistors,” in VLSI Symp. Tech. Dig., Jun. 2000, pp. 174–175.

[9] H. C. Pao and C. T. Sah, “Effects of diffusion current on characteristics of metal-oxide (insulator)-semiconductor transistors,” Solid State Electron., vol. 9, no. 10, pp. 927–937, Oct. 1966.

[10] B. Yu, J. Song, Y. Yuan, W. Lu, and Y. Taur, “A unified analytic drain-current model for multiple-gate MOSFETs,” IEEE Trans. Electron Devices, vol. 55, no. 8, pp. 2157–2163, Aug. 2008.

[11] Duarte, J.P Sung-Jin Choi,Dong-Il Moon,Jae-Hyuk Ahn, “A Universal Core Model for Multiple-Gate Field-Effect Transistors. Part I: Charge Model,” IEEE Trans. Electron Devices, vol.60,no. 2, pp. 840–848, Feb. 2013.

[12] Duarte, J.P Sung-Jin Choi,Dong-Il Moon,Jae-Hyuk Ahn, “A Universal Core Model for Multiple-Gate Field-Effect Transistors. Part II: Drain Current Model,” IEEE Trans. Electron Devices, vol.60,no. 2, pp. 848–854, Feb. 2013.

[13] A. Tsormpatzoglou, C. Dimitriadis, R. Clerc, G. Pananakakis, and G. Ghibaudo, “Semianalytical modeling of short-channel effects in lightly doped silicon trigate MOSFETs,” IEEE Trans. Electron Devices, vol. 55, no. 10, pp. 2623–2631, Oct. 2008.

[14] Y. W. Jin, C. Zeng, L. Ma, and D. Barlage, “Analytical threshold voltage model with TCAD simulation verification for design and evalution of tri-gate MOSFETs,” Solid State Electron., vol. 51, pp. 347–353, Mar. 2007.

[15] K. Akarvardar, A. Mercha, S. Cristoloveanu, P. Gentil, E. Simoen, V. Subramanian, and C. Claeys, “A two-dimensional model for interface coupling in triple-gate transistors,” IEEE Trans. Electron Devices, vol. 54, no. 4, pp. 767–775, Apr. 2007.

[16] Xin Sun, Tsu-Jae King Liu, “Scale-Length Assessment of the Trigate,” IEEE Trans. Electron Devices, vol. 56, no. 11, pp. 2840–2842, Nov. 2009.

[17] K. K. Young, "Short-channel effect in fully-depleted SOI MOSFETs," IEEE Trans. Electron Devices, vol. 36, no. 2, pp. 399–402, Feb. 1989.

[18] Atlas User's Manual, Device Simulation Software, Silvaco, Santa Clara, CA,2008, software ver, vol. 5, no. 0.